

## THREE-DIMENSIONAL MODELING OF HYDRODYNAMIC AND FLUSHING IN DEEP BAY

Joseph Hun-Wei LEE & Aiguo QIAN  
Department of Civil Engineering, University of Hong Kong, Pokfulam Road,  
Hong Kong, E-mails: hreclhw@hkucc.hku.hk, agqian@hkusua.hku.hk

**Abstract:** Hydrodynamic flushing in estuaries is an important linkage between hydrodynamic and water quality processes. For the simulation of flushing of local areas, three-dimensional (3D) hydrodynamic modeling is required for predicting flows induced both by barotropic and baroclinic gradients. In this study for Deep Bay, Hong Kong, a 3D hydrodynamic model was firstly calibrated and verified using field survey data in dry season and wet season. The flow in the bay is relatively well-mixed with weak vertical salinity gradients, and follows mainly the bottom topography. The flushing feature was quantified via a systematic numerical experiment. It is demonstrated that the flushing rate is in the order of 0.05 per day in the inner bay, and is significantly affected in both the dry and wet season by salinity gradients.

**Key words:** Hydrodynamic modeling, Estuarine circulation, Salinity, flushing, Deep Bay

### 1. INTRODUCTION

Deep Bay is a large shallow semi-enclosed bay located on the east bank of the Pearl Estuary (Fig.1). It is surrounded by Shenzhen in the north and the New Territories of Hong Kong in the south. In recent years, due to rapid urbanization and increasing pollution load, there has been notable deterioration of water quality in the bay. Regular marine water quality monitoring in Deep Bay has suggested a continuation of this trend (EPD 2000, 2001); the measurements showed highly unsatisfactory Dissolved Oxygen, E.Coli, and nutrient concentrations, suggesting serious eutrophication conditions. The potential long-term pollution threatens the sensitive ecosystems (wetland reserves) and oyster culture in the bay. Despite the escalating pollution loads and the general eutrophic level, there has been few reports of algal blooms and red tides in Deep Bay. An understanding of the flushing characteristics in the bay is a first step towards the study of water quality and ecosystem response in this important water body.

Hydrodynamic flushing feature in an estuary is a measure of its self-purification capability; it determines the renewal of “clean ocean water” and hence the water quality evolution. Conventionally, estuarine flushing time (conversely flushing rate) is computed by simplified approaches, such as the tidal prism or salt balance method (Fischer 1979; Ippen 1966; Officer 1991; Lee 2003). These methods typically assume full mixing and cannot account for spatial variations; they are also not applicable when no salinity data is available, or in bays with weak salinity gradients. For example, Burwell et al. (1999) presented the bay wide residence time distribution in their study on Tampa Bay. A systematic procedure to determine numerically the flushing and carrying capacity of mariculture zones in Hong Kong using 3D modeling has also been recently proposed (Lee and Choi 2001, 2003). This involves the computation of the 3D flow, and accurate determination of flushing time from a numerical tracer experiment by solving the mass transport equation. In a preliminary assessment of eutrophication status of Deep Bay (Qian et al 2002), it is observed that there is serious nutrient enrichment in the

inner bay where flushing is weak but there is general compliance with water quality standards in the outer bay where flushing is strong.

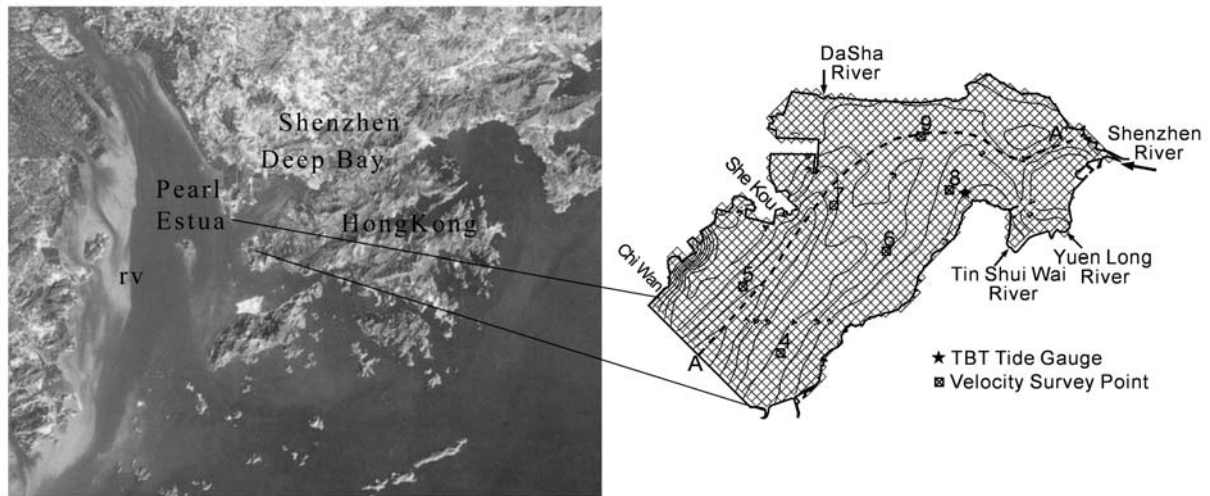


**Fig. 1** Deep bay and adjoining pearl estuary

To better understand the water quality evolution in Deep Bay, we have carried out a study of its flushing characteristics. As the flow is driven by astronomical tides and density stratification, and affected by complicated boundaries, a robust 3D hydrodynamic model that accounts for the integrated effects is particularly necessary to simulate the local flushing (Jirka & Lee 1994; Lee and Choi 2001, 2003). The computed flow and salinity distribution are in satisfactory agreement with field measurements.

## **2. THREE-DIMENSIONAL HYDRODYNAMIC MODELING OF DEEP BAY**

### **2.1 MODEL DESCRIPTION**

The Environmental Fluid Dynamic Code (EFDC) developed at the Virginia Institute of Marine Science is adopted in our study (Hamrick 1992). The model solves the 3D, vertically hydrostatic, free surface equations of motion, together with continuity and mass balance equations. It responds to surface wind stress, heat and salinity fluxes, freshwater discharge, and specification of tidal forcing. Three-dimensional transport equations for the turbulent intensity and length scale as well as temperature, salinity, dye tracer, and suspended sediment are solved simultaneously. A second-moment turbulence closure model is solved to provide the vertical turbulent eddy viscosity in the model (Mellor and Yamada 1982). Horizontal diffusion is calculated using the Smagorinsky formula. The model uses Cartesian or boundary-fitted curvilinear-orthogonal coordinates in the horizontal plane and a sigma-stretched coordinate system in the vertical direction. The computational scheme uses an external-internal mode splitting to solve the horizontal plane momentum equations and the continuity equation on a staggered grid, using a combination of finite volume and finite difference techniques (Hamrick 1992; Hamrick and Wu 1996).

### **2.2 DATA OF DEEP BAY FOR MODEL CALIBRATION AND VERIFICATION**

The model is calibrated and validated against two sets of full-tidal cycle field observations. The surveys were carried out in March (dry season) and August (wet season) 1996 (Hyder Consultants 1996). Basically, the tide during the wet season survey can be identified as mainly semi-diurnal whereas the tide during the dry season was mainly diurnal; both surveys were performed under neap tide conditions. The relevant water level, velocity, and salinity data at a number of key survey stations (Fig.1) were used for model validation. Corresponding

wind stress and water temperature variation were omitted due to their negligible effects during the survey period.

### **2.3 MODEL GRID AND BOUNDARY CONDITIONS**

The model grid was constructed in a rectangular and vertical sigma-stretched coordinate system. It contains 1468 cells in the horizontal plane (Fig.1). The grid cell size was 250m by 250m. 5 uniformly spaced layers were specified in the vertical direction.

There are 4 river discharges along northeast inner bay (Fig.1) and the open boundary is located at the southwest bay entrance adjoining the Pearl Estuary. As the river discharges are all relatively small, they are treated as point sources. Since the effect of the Pearl Estuary on flows in Deep Bay is complex, a calibrated Pearl Estuary model (Delft3D) was used to generate the open boundary conditions, including water level and salinity distribution along the boundary cross section. The Pearl River Estuary model covers the entire Pearl Estuary including Hong Kong and all the islands, and extends sufficiently into the South China Sea. This larger model is driven by tidal forcing (nine tidal constituents and observed long term average salinity) at its open boundaries. The Pearl Estuary model has been extensively calibrated and verified against field data in Hong Kong waters (Lee and Qu 2003).

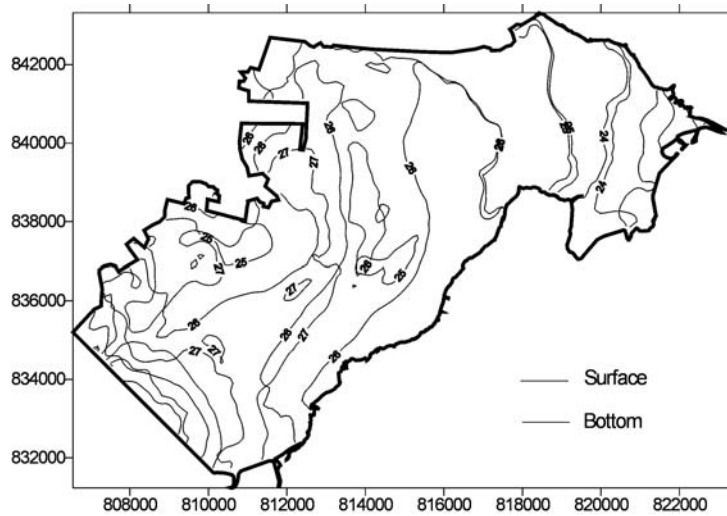
### **2.4 NUMERICAL MODEL RESULTS**

The model was calibrated for Deep Bay using the dry season data set. Using the open boundary water surface elevation and salinity distribution derived from Pearl Estuary model, a 2.5 cm roughness height was used to parameterize bottom friction. In general the agreement between predicted and measured water level and velocity (not shown) is satisfactory. Computed salinity distributions also agree with the measurements. The general well mixed salinity of the dry season is well produced (see Fig.2a). Fig.2b gives the computed flow field of the bay.

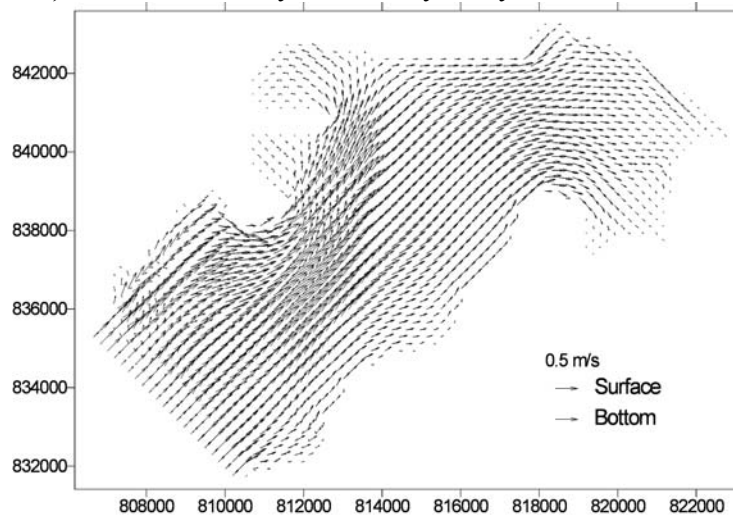
The calibrated model is verified using the wet season data in 1996. For this case, the semi-diurnal circulation and the measured weak salinity stratification are well reproduced. Fig.3a shows the measured versus the computed velocity magnitudes and directions near the surface and near the bed. The measured velocities are rather characteristic for a well mixed/weakly stratified estuary. The difference between surface and bed velocities is relatively small for the survey stations. Currents generally flow northeast during rising tide when the bay is filled. During falling tide, when the bay is emptied, the currents direct to the southwest; the maximum speed is around 0.5 m/s. The simulated velocity field (Fig.2b) also reveals some flow patterns in the bay: 1) Velocity magnitude near north side is slightly larger than near south side, which conforms to the measurements of 6 key survey stations. 2) As seen in Fig.1, the Shekou cape at middle of north side forms the narrowest cross section in the bay, and there is a small deep channel from the cape to the mouth of the bay, the main longitudinal current direction hence follows along this channel. Due to the effect of density stratification, the directions of current between channel surface and its bottom exhibit some difference as shown in Fig.2b. 3) Behind the Shekou cape are two small coves between the cape and the post-reclamation coastline of Shenzhen side (see Fig.1). The velocities in these two coves are distinctively small and there are vortices formed during flooding tidal phase. This will result in the deposition of sediment and the accumulation of other substance carried into the coves. Dasha River from Shenzhen flows perpendicularly into the north cove (Fig.1), this to an extent fences out the inflow of ebb current and hence weakens the flow in the cove. Therefore, the impact of Dasha River is mainly to input more wastes to the cove source rather than enhance its flushing. 4) Generally the flows along south side are relatively smooth which conforms to its smooth shoreline.

With the salinity distribution at open boundary provided by Pearl Estuary model, the calibrated model well predicted the salinity situation. The measured versus computed salinity

time series and spatial distribution are shown in Fig.3. In general, the magnitude of the computed salinities is in agreement with the measurements; as seen from the comparison of surface and bottom salinity distribution, the degree of stratification in the bay is well-predicted by the model.



a) Well mixed salinity in inner bay in dry season, flood tide



b) Peak Flood Flow

Fig. 2 Computed Velocity and Salinity Fields in Deep Bay, Dry Season

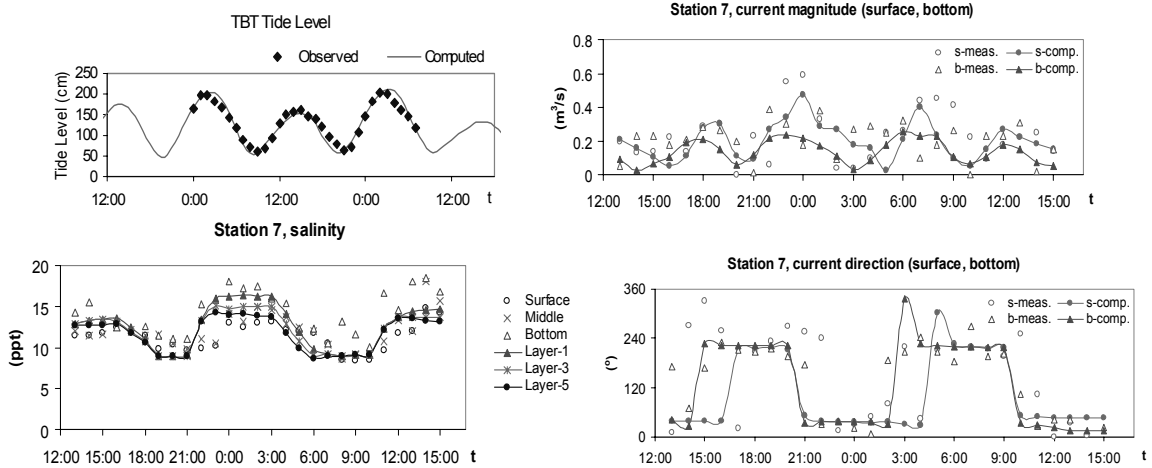
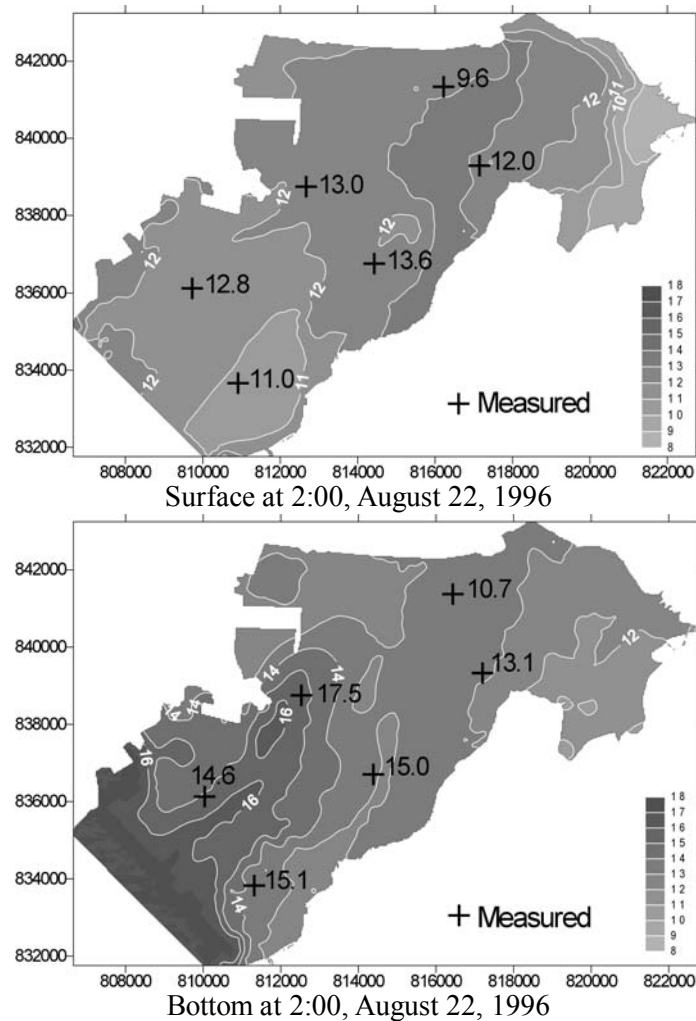


Fig. 3-a Comparison of Measured and Computed Tides and Current (August 21-22, 1996), Wet Season



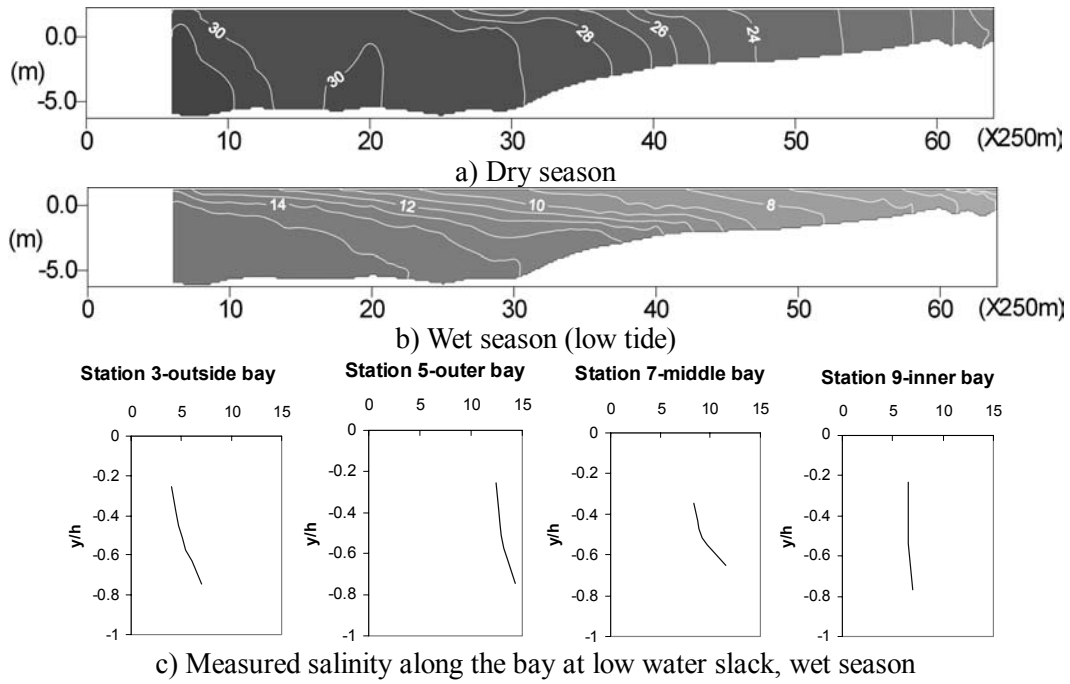
**Fig. 3-b** Comparison of Measured and Computed Salinity Distribution, Wet Season

Fig.4 shows the computed and measured typical salinity longitudinal transect through the bay in wet season, and a typical dry season situation is also given for comparison. The transect is taken basically along the deepest depths in the bay (see Fig.1) and conforms to the main current direction.

As seen from the figure, the largest vertical salinity gradient occurs at the middle part, with a relatively steep bed slope. The vertical salinity structure along the bay is generally reproduced (see Fig.4b and 4c). The salinity gradient in the bay, resulted from the mixing of the Pearl Estuary saline intrusion with freshwater, significantly influences the flushing of the bay.

### 3. MODELING OF TIDAL FLUSHING

Based on the validated hydrodynamic model, a numerical dye tracer experiment is performed. The entire bay is initially labeled (at high water) at a uniform 100 percent concentration with a passive tracer at time  $t=0$ . The subsequent change in the tracer mass in different parts of the bay is then tracked by solving the 3D mass transport equation. At the open boundary, the inflow tracer dye concentration is 0. Four typical tidal conditions (spring tide and neap tide in dry season and wet season) are computed. The computed mass removal for a given segment or part of the bay can typically be fitted by a double exponential decay curve (Lee and Choi 2001). The computed flushing time is taken as the time when mass removal falls below  $1/e$  of the original vertically integrated mass.



**Fig. 4** Typical A-A' Longitudinal Transect Salinity

To compute the different flushing feature in Deep Bay, the entire bay water was grouped into 5 segments as seen in Fig.5a. Shenzhen River, Yuen Long River and Tin Shui Wai River are included in segment 1. Dasha River flows into segment 3. Using the typical tidal and associated salinity conditions, the flushing time was calculated as shown in Table 1 and Fig.5.

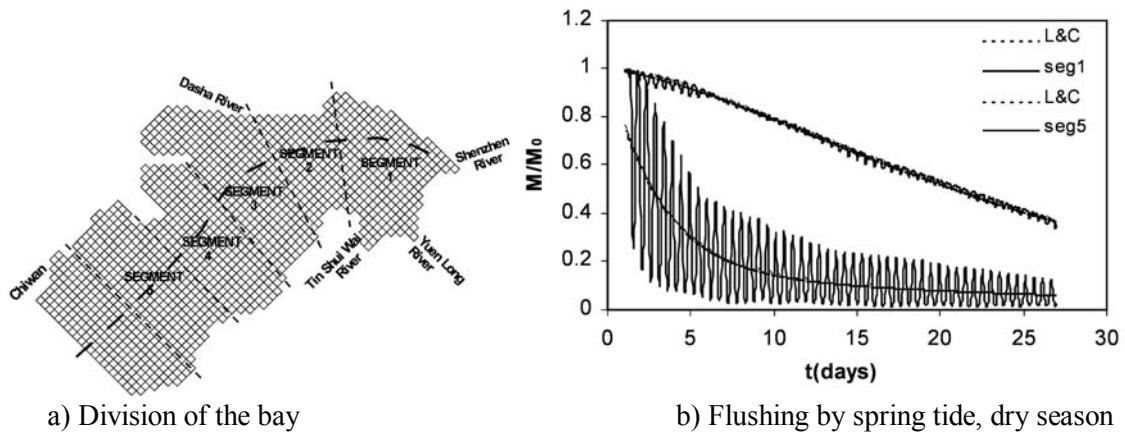


**Fig. 5** Computation of Flushing Time

Table 1 Flushing Time in Deep Bay (system-wide, days)

	Segment 5	Segment 4	Segment 3	Segment 2	Segment 1
Spring tide--(dry)	4.1	12.6	20.5	24.3	26.5
Spring tide--(wet)	6.2	14.8	26.5	26.3	25.7
Neap tide--(dry)	6.0	15.0	24.7	27.5	28.0
Neap tide--(wet)	4.0	14.1	25.2	24.5	24.2
Average	5.1	14.1	24.2	25.7	26.1
Comparison: Spring tide--no salinity	10.7	19.2	32.1	36.0	27.0

*Computation Conditions:* 1) Tide: M2; tide range: spring 2.1m and neap 1.0m for Hong Kong waters. 2) Dry season: salinity at open boundary: vertically uniform, 26 ppt both at both surface and bottom; total freshwater discharge: 6.22 m<sup>3</sup>/s. 3) Wet season: salinity at open boundary: vertically linear distribution, 8 ppt at surface and 16 ppt at bottom; total freshwater discharge: 13.7 m<sup>3</sup>/s.

In the results presented in Table 1, the flushing is also studied for the case of zero salinity gradient. It is found that the contribution of salinity to the flushing time is generally about ¼ of the total. In the absence of any vertical salinity gradient, the flushing of segment 2 and 3 is significantly weaker than that with vertical density stratification; the corresponding differences is very small for segment 1 due to the river discharges. The difference of flushing time in spring tide and neap tide is small, but the amplitude during a cycle in spring tide is larger than that in neap tide due to the larger velocity of spring tide. In dry season, the direct contribution of freshwater discharge is limited so that there is a flushing gradient from inner to outer portion. In wet season, the larger freshwater inflow results in a slightly greater flushing of innermost of the bay (segment 1) compared with the next seaward segment.

The computed flushing time within Deep Bay ranges from 26.1 days in inner bay to 5.1 days in outer part – i.e. the flushing rate (inverse of flushing time) in the innermost of Deep Bay is only 0.04 per day. Compared to typical net algal growth rates of the order of 0.1 per day, the weak flushing would permit the accumulation of nutrients and algal blooms. However, the flushing rate along the bay rapidly increases to 0.2 at the outer end. Compared to land-locked tidal inlets in Eastern Hong Kong waters (e.g. Tolo Harbour), the flushing of outer Deep Bay is relatively good. This appears to explain why red tides scarcely occur in Deep Bay compared to frequently occurrences in Tolo Harbour. In addition, the high suspended solids concentration in the bay leads to significant attenuation of the photosynthetically active radiation (PAR), which would render the bay more light-limited for algal growth (Qian, Lee and Wang 2002).

#### 4. CONCLUDING REMARKS

A 3D hydrodynamic model has been applied to compute the 3D circulation in Deep Bay. The model results for both the dry and wet seasons are in good agreement with field observations. The flushing in Deep Bay is significantly affected by both vertical and longitudinal salinity gradients; computed flushing time varies from 15-28 days in the bay proper to around 5 days near the ocean boundary. In particular, the flushing rate in the innermost part of Deep Bay is 0.04 per day, a condition which can favor algal blooms to develop.

#### ACKNOWLEDGMENTS

This study is supported by a grant under the National Natural Science Foundation of China (NSFC) /Hong Kong Research Grants Council (RGC) joint research scheme.

#### REFERENCES

- Blumberg, A.F., and Mellor, G.M. (1987). "A description of a three-dimensional coastal ocean circulation model." *Three-dimensional coastal ocean models, coastal and estuarine Sci.*, N.S.Heaps, ed., Vol. 4, American Geophysical Union, Washington, D.C., 1-19.
- Burwell, D., Vincent, M., Luther, M., Galperin, B., (1999). "Modeling Residence Times: Eulerian vs Lagrangian", *Estuarine and Coastal Modeling, Proceedings of the Sixth International Conference*, Nov. 3-5, 1999, New Orleans, Louisiana.
- EPD, (2001). *Marine Water Quality in Hong Kong in 2001*. Hong Kong.
- Fischer, H.B., List, E.J., Koh, R.C.Y., Imberger, J. and Brooks, N.J., (1979), *Mixing in Inland and Coastal Waters*, Academic Press, San Diego, California.

- Harmrick, J.M. (1992). "Three-dimensional environmental fluid dynamics computer code: Theoretical and computational aspects." *Spec. Rep. In Appl. Marine Sci. and Oc. Engrg., No. 317*. College of William and Mary, Virginia Inst. of Marine Science, Va.
- Harmrick, J.M. (1996). "User's manual for the environmental fluid dynamics computer code." *Spec. Rep. In Appl. Marine Sci. and Oc. Engrg.*, Virginia Inst. of Marine Science, Va.
- Hyder Consulting Ltd. & CES (Asia) Ltd., 1998. Deep Bay Water Quality Regional Control Strategy Study-Regional Water Quality Management Strategy Options," *Final Report*.
- Ippen, A.T. (1966). *Estuary and Coastline Hydrodynamics*. McGraw-Hill, New York.
- Jirka, G.H. and Lee, J.H.W. (1994). Waste disposal in the ocean. *Water quality and its control*, Balkema. 193-242.
- Lee, J.H.W., Choi, K.W. and Arega, F. (2003). "Environmental management of marine fish culture in Hong Kong," *Marine Pollution Bulletin*, Volume 47, Issues 1-6, January-June.
- Lee, J.H.W., Choi, K.W., Arega, F. and Qu, B. (2001). "Environmental management of mariculture in Hong Kong," *Technical Report*, The university of Hong Kong, Hong Kong.
- Lee, J.H.W and Qu, B. (in press). "Hydrodynamic tracking of the massive spring 1998 red tide in Hong Kong", *Journal of Environmental Engineering*, ASCE.
- Officer, C.B. and Kester, D.R. (1991), "On estimating the non-advective tidal exchanges and advective gravitational circulation exchange in an estuary", *Estuarine, Coastal and Shelf Science*, Vol. 32.
- Qian, A.G., Lee, J.H.W. and Wang, Z.Y. (2002). "Hydrodynamic and Eutrophication Modeling of Deep Bay." *Presentation*, The Second International Workshop on Coastal Eutrophication, Tianjin University.